www.rericjournal.ait.ac.th

A Study on Paddy Drying with an Automated Fluidized Bed Dryer

Autchara Junphong*, Ninlawan Chaitanoo*, Apidet Sangsamoot+, Natthamon Thamon+, Thongchai Tanasombat+, Penwarat Panphattharachai#, and Atchara Chaiya*[1]

Abstract – *This study presents the development and performance evaluation of an automated fluidized bed dryer for paddy, equipped with a microcontroller-based system (Arduino) for precise control of temperature and humidity. The dryer, with dimensions of 47 cm× 72 cm × 190 cm, was fitted with sensors at the inlet, middle, and outlet of the grain column. Drying experiments were conducted at temperatures of 40, 50, and 60°C for 60, 90, and 120 minutes, using 1,500 grams of paddy with an initial moisture content ranging from 14% to 15%w.b. The optimal air velocity for fluidization was found to be 9.67 m/s, ensuring stable grain suspension and improved heat and mass transfer. The condition of 60°C for 120 minutes yielded the highest moisture reduction of 70.62% (final moisture content 4.22% w.b.) with moderate energy use (SEC = 27.37 MJ/kg). This condition demonstrated a well-balanced trade-off between drying efficiency and energy consumption, making it suitable for real-world applications in medium-scale farms or small-scale agro-industrial facilities where both product quality and energy performance are critical, while also contributing to global efforts in sustainable energy use.*

Keywords – Fluidize Bed, Moisture, Paddy Drying, Arduino, SDG7.

1. INTRODUCTION

Recent advances in agricultural drying technologies have significantly improved postharvest handling and food preservation, while also aligning with global sustainability targets such as SDG 7: Affordable and Clean Energy. Various mechanical dryers, such as rotary dryers, tray dryers, recirculating batch dryers, and solar-assisted hybrid dryers, have been employed to address the limitations of traditional sun drying [1]-[2]. Each method offers trade-offs in terms of energy consumption, drying time, and product quality. For example, tray dryers provide uniform drying for small-scale operations but often consume more energy and require longer drying cycles. Rotary dryers, on the other hand, offer continuous drying for large volumes but may lead to non-uniform moisture content due to rotational tumbling [3].

Among these, fluidized bed drying has emerged as a highly efficient method due to its rapid heat and mass transfer, low drying time, and suitability for particulate agricultural materials. This technique uses high-pressure hot air to suspend and fluidize the product, ensuring uniform temperature distribution and moisture removal. Research by Luthra and Sadaka [4], Wazed *et al*. [5], and Kwanchai [6] confirms the effectiveness of this method in preserving grain integrity and improving head rice yield compared to conventional methods.

Automation technologies have further elevated the efficiency and precision of drying systems. The integration of microcontroller-based platforms such as Arduino enables smart control of temperature, humidity, and drying time. These systems are cost-effective, programmable, and scalable, allowing real-time monitoring and control via IoT-based interfaces. Studies by Nebrida [7] and Herani *et al* [8], show that Arduino-controlled dryers can maintain target drying conditions with high accuracy while significantly reducing energy consumption and labor requirements—an approach that directly supports the energy efficiency targets outlined in SDG 7.

Paddy, as a major agricultural product in Southeast Asia, particularly benefits from such technological improvements. Typically harvested at high moisture content (~20–30%, wet basis), paddy must be dried to around 13–14% to ensure safe storage and prevent spoilage [9]. Traditional sun drying is common but limited by weather dependency and inconsistency. The adoption of mechanical drying systems addresses these issues, with fluidized bed dryers offering a viable alternative. Moreover, energy performance, often evaluated through Specific Energy Consumption (SEC), has become a critical metric. Optimized fluidized bed dryers have demonstrated SEC values suitable for small and medium-scale applications, thereby promoting the use of affordable, reliable, and modern energy solutions in rural agricultural communities [3]-[4], [6].

This study thus focuses on the development of an Arduino-controlled fluidized bed dryer aimed at improving the drying efficiency of paddy. It seeks to

DOI: https://doi.org/10.64289/iej.25.03A11.7634243

*Faculty of Engineering, Rajamangala University of Technology Lanna 128 Huay Kaew Road, Mueang, Chiang Mai, 50300, Thailand.

+Faculty of Engineering, Rajamangala University of Technology Lanna Lampang 200 Moo 17, Mueang, Lampang, Lampang, 52000, Thailand.

#College of Integrated Science and Technology, Rajamangala University of Technology Lanna 98 Moo 8, Papong, Doisaket, Chiang mai, 50220, Thailand.

[1]Corresponding author;
Tel: +6687 361 6203
E-mail: atchara_c@rmutl.ac.th

evaluate the operational performance, energy savings, and applicability of this system in rural agricultural settings, contributing to the broader advancement of accessible and sustainable postharvest technologies in line with SDG 7.

2. RESEARCH METHODOLOGY

The methodology of paddy drying using an automated fluidized bed dryer, in which temperature and humidity are controlled automatically via Arduino IDE. The operation process is systematically outlined as shown in Figure 1.

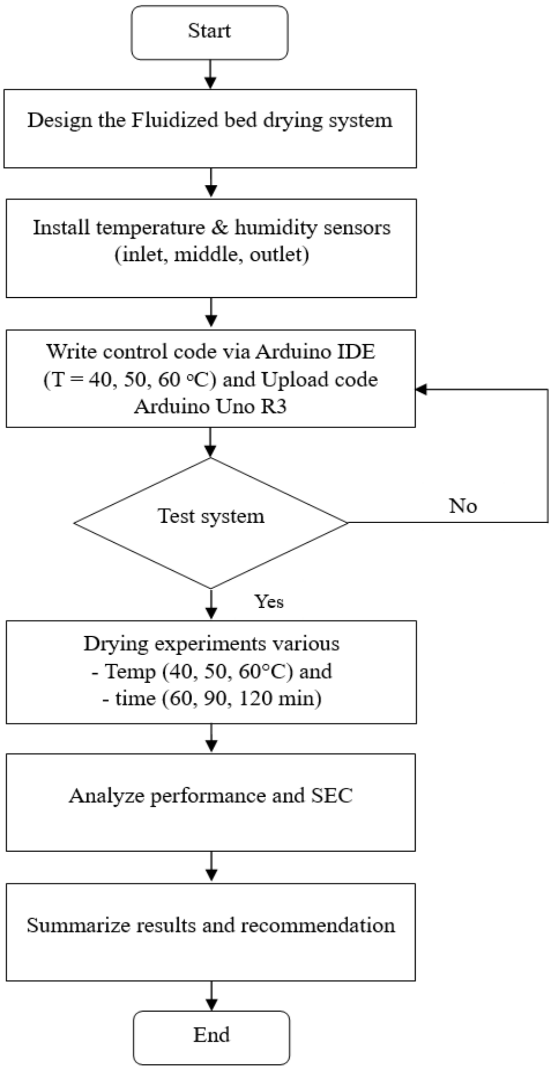

Fig. 1. Flow diagram of the automated.

2.1 Design Concept of an Automated Fluidized Bed Dryer

The conceptual design of an automated fluidized bed dryer aims to develop a high-efficiency drying system for paddy or other agricultural materials. The system is intended to support precise real-time control of temperature, humidity, and drying duration while maintaining cost-effectiveness and practical usability for community-level or small-scale industrial operations as shown in Figure 2.

2.1.1 System structure

The drying system is designed as an integrated assembly of mechanical and thermal components working in synergy to achieve efficient moisture removal from paddy. Each component serves a specific role in controlling airflow, heat transfer, and uniform fluidization of grains. The overall structural configuration is optimized to ensure energy efficiency, operational stability, and consistent drying quality, while also allowing flexibility in material selection and scalability for various operational capacities. The primary subsystems are as follows:

1) Drying Chamber: A vertically oriented cylindrical chamber made from stainless steel or poly vinyl chloride (PVC), selected for its heat resistance.
2) Distributor Plate: Installed at the base of the drying chamber, this perforated plate ensures uniform hot air distribution to facilitate consistent fluidization of the grain bed.
3) Blower (Fan): Supplies forced air through the heater into the drying chamber at a velocity sufficient to achieve fluidization of paddy grains.
4) Electric Heater: Heats incoming air to a controlled temperature in the range of 30–70°C before it enters the drying chamber.

2.1.2 Automation and control system

The system employs a microcontroller-based platform to coordinate heating, airflow, and monitoring functions. Key components include:

1) Arduino Uno or ESP32 Board: Serves as the main controller for all components, including the heater, blower, alert systems, and data display.
2) Temperature Sensors (e.g., DS18B20 or DHT22): Installed at three critical points in the system—air inlet, chamber center, and outlet—to monitor thermal conditions throughout the drying process.
3) Humidity Sensor (Capacitive RH sensor): Measures the relative humidity of the circulating air inside the chamber to assess moisture removal.
4) Relay Module: Controls the on-off switching of the heater and blower according to programmed conditions.
5) Liquid Crystal Display (LCD) or Organic Light-Emitting Diode (OLED) display: Provides real-time visualization of system parameters, including temperature, relative humidity, and remaining drying duration.
6) Data Logging System (SD Card or IoT Platform): Records operational data from each drying cycle for performance analysis and potential remote monitoring.

©2025. Published by RERIC in International Energy Journal (IEJ), selection and/or peer-reviewed under the responsibility of the Organizers of the **"17th International Conference on Science, Technology and Innovation for Sustainable Well-Being (STISWB 2025)"** and the Guest Editor: Prof. Pradit Terdtoon of Chiang Mai University, Chiang Mai, Thailand.
www.rericjournal.ait.ac.th

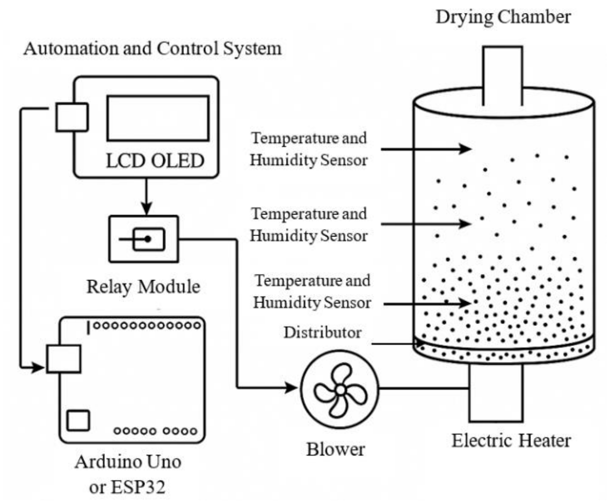

Fig. 2. Design concept of an automated fluidized bed dryer.

2.1.3 Operating principles

The drying process follows a controlled sequence to ensure efficient heat transfer, uniform grain fluidization, and consistent moisture reduction. The operational steps are:

1) System Initialization: The user activates the system and sets the target temperature and drying duration via a manual switch.
2) Startup Control: The Arduino microcontroller powers the blower and heater until a preset temperature is reached.
3) Fluidization Phase: Paddy grains are suspended above the distributor plate, maintaining continuous fluidization throughout drying.
4) Temperature Regulation: A PID control algorithm sustains the drying temperature within the designated range to enhance process stability and efficiency.
5) Cycle Completion: Upon reaching the set time, the system shuts down automatically, concluding the drying operation.

2.2 Design and Construction of the Automated Fluidized Bed Dryer

The dryer was constructed to translate the functional requirements outlined in Section 2.1 into a robust and operational prototype. The design prioritizes structural stability, efficient heat and mass transfer, and precise process control. Materials and dimensions were selected to balance durability, manufacturability, and performance under varying operating conditions. The following subsections detail the major construction components.

1) The drying column used to be 15 cm in diameter and 100 cm high. A column support flange was fabricated with an outer diameter of 20 cm and an inner diameter of 17.5 cm.
2) The heating unit of the automated fluidized bed dryer was designed using a 6-inch diameter pipe, with six 10 mm holes drilled on both the upper and lower surfaces to accommodate the installation of 1,300-watt electric coils as the heat source. A blower functions as the air supply, directing airflow through the heating unit to generate hot air for the drying process.
3) The control system was integrated at three key locations along the column—namely, the inlet, the middle section, and the outlet—as well as at the heating unit. Sensors were installed to measure temperature and relative humidity (%RH), enabling real-time monitoring and automatic regulation of the heating element based on predefined setpoints.

2.3 Programming the Control System

The control algorithm, developed within the Arduino Integrated Development Environment (IDE), implemented precise thermal regulation to maintain target temperatures of 40°C, 50°C, and 60°C with stringent accuracy as shown in Figure 3. The system incorporated automated thermal cutoff protocols that ceased heating operations upon achieving the predetermined setpoint, thereby preventing temperature overshoot and ensuring optimal energy efficiency. Concurrent monitoring of relative humidity (%RH) was executed at three strategically positioned measurement points: the inlet, intermediate section, and outlet, enabling comprehensive spatial analysis of moisture distribution throughout the experimental apparatus. The compiled firmware was subsequently deployed to an Arduino UNO R3 microcontroller platform, facilitating real-time process control and data acquisition with microsecond-level temporal resolution.

2.4 Experiments

The experimental program was designed to evaluate the operational performance of the automated fluidized bed dryer under controlled conditions. Two primary investigations were carried out: the determination of optimal air velocity for stable fluidization and the assessment of drying performance under varying thermal and temporal settings. The following subsections describe the procedures for air velocity measurement and drying experiments in detail.

2.4.1 Air velocity determination

To determine the appropriate air velocity for fluidization, the blower speed was incrementally adjusted across five levels while maintaining the drying air temperature at 50°C. The speed was gradually increased until a 1,500 g sample of paddy rice achieved uniform fluidization, characterized by consistent particle suspension throughout the drying chamber. The corresponding air velocity was then measured and recorded using a calibrated anemometer.

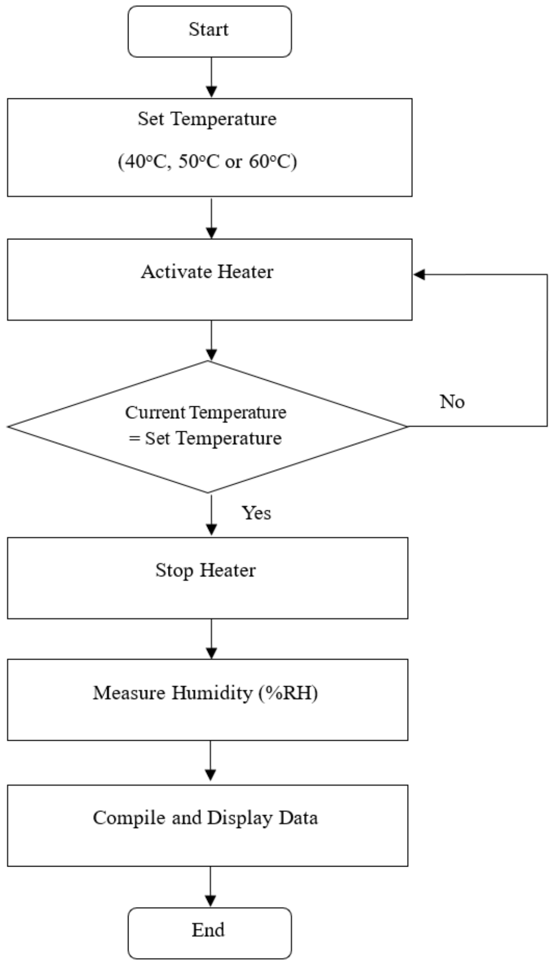

Fig. 3. Flow diagram of Arduino-based thermal control system for fluidized bed dryer.

2.4.2 Drying procedure

Drying experiments were conducted to investigate the effects of drying temperature, relative humidity, and duration on drying performance and grain quality. The experimental protocol was as follows:

1) A 1,500 g sample of freshly harvested paddy rice was weighed and loaded into the vertical drying column.
2) The system was programmed to operate at three target temperatures: 40°C, 50°C, and 60°C, with corresponding drying durations of 60, 90, and 120 minutes.
3) Initial values for grain weight, ambient temperature, and relative humidity (%RH) were recorded. During each drying run, temperature and humidity data were collected at 5-minute intervals from three sensor positions within the drying column—namely, the air inlet, the middle section, and the outlet.
4) Upon completion of each drying cycle, the final weight of the rice sample was measured, and the final moisture content was determined using a Moisture Analyzer (Model MB25, OHAUS™), or moisture content during drying can be estimated using Equation 1:

$$MC_{w.b.} = [w_w / (w_w + w_d)] \times 100\% \quad (1)$$

where $MC_{w.b.}$ denotes the moisture content on a wet basis, w_w represents the mass of water in kilograms, and w_d refers to the dry mass of the material in kilograms.

Additionally, the convective heat transfer involved in the drying process can be described using Equation 2:

$$Q = hA(T_{air} - T_{surface}) \quad (2)$$

where Q is the heat transfer rate in kilowatts (kW), h is the convective heat transfer coefficient in watts per square meter per degree Celsius (W/m²·°C), A is the surface area in square meters (m²), T_{air} is the temperature of the air in degrees Celsius (°C), and $T_{surface}$ is the temperature of the grain surface in degrees Celsius (°C).

The convective heat transfer coefficient (h) quantifies the efficiency of heat exchange between a surface and a moving fluid. It depends on fluid properties and flow conditions, and is typically estimated using dimensionless numbers such as Nu, Re, and Pr, via:

$$h = Nu \cdot k/L \quad (3)$$

where k is the thermal conductivity of the fluid, and L is the characteristic length. The Nusselt number itself is often derived from correlations such as the Dittus–Boelter equation for turbulent flow in pipes:

$$Nu = 0.023Re^{0.8}Pr^{n} \quad (4)$$

with n = 0.4 for heating of fluid
n = 0.3 for cooling of fluid

where Re is the Reynolds number ($Re = \rho uD/\mu$), and Pr is the Prandtl number ($Pr = c_p/\mu k$), which account for flow regime and fluid properties, respectively [9]. These correlations are widely validated and applied in various thermal engineering applications, particularly in internal flows and heat exchanger design.

2.5 Energy Performance Evaluation

Specific Energy Consumption is a key performance indicator used to evaluate the energy efficiency of drying systems. It is defined as the amount of energy consumed to evaporate one kilogram of water from the material being dried. This value reflects both the thermal and electrical energy input of the system relative to the moisture removed and is especially important when assessing the viability of drying technologies for high-moisture-content agricultural products. The SEC is calculated using the following equation:

$$SEC = E/m_w \quad (5)$$

where SEC denotes the specific energy consumption in megajoules per kilogram of water evaporated (MJ/kg of water), E represents the total energy input from the blower and electric heater in megajoules (MJ), and m_w is the mass of water evaporated in kilograms (kg).

This method is commonly applied in drying systems such as swirl-fluidized bed dryers, which are designed for materials with high surface moisture. Studies indicate that SEC is an effective metric for comparing energy efficiency across different drying conditions, airflow rates, and temperature settings [10].

3. RESULTS AND DISCUSSION

This research project aimed to develop an automated fluidized bed dryer for paddy that enables precise temperature control through Arduino IDE-based programming. The initiative represents an interdisciplinary integration of drying technology and automated control systems within an engineering framework. The ultimate goal was to construct a functional prototype capable of effectively reducing the moisture content of paddy while ensuring high energy efficiency.

3.1 Design Results of the Automated Fluidized Bed Paddy Dryer

For the engineering design phase, the researchers employed SolidWorks software to construct a prototype dryer comprising four main components: a blower, a heating unit, an airflow control valve, and a fluidized bed column equipped with temperature and relative humidity sensors at three distinct locations, as illustrated in Figure 4. The design process was conducted in accordance with relevant standards and engineering considerations.

A critical aspect of this research was the design of the gas distribution system, which directly influences fluidization quality as well as heat and mass transfer efficiency. Key design parameters included orifice size, void fraction, airflow velocity, and the height-to-diameter (H/D) ratio of the column. These factors play a significant role in achieving uniform air distribution and maintaining consistent drying performance [11].

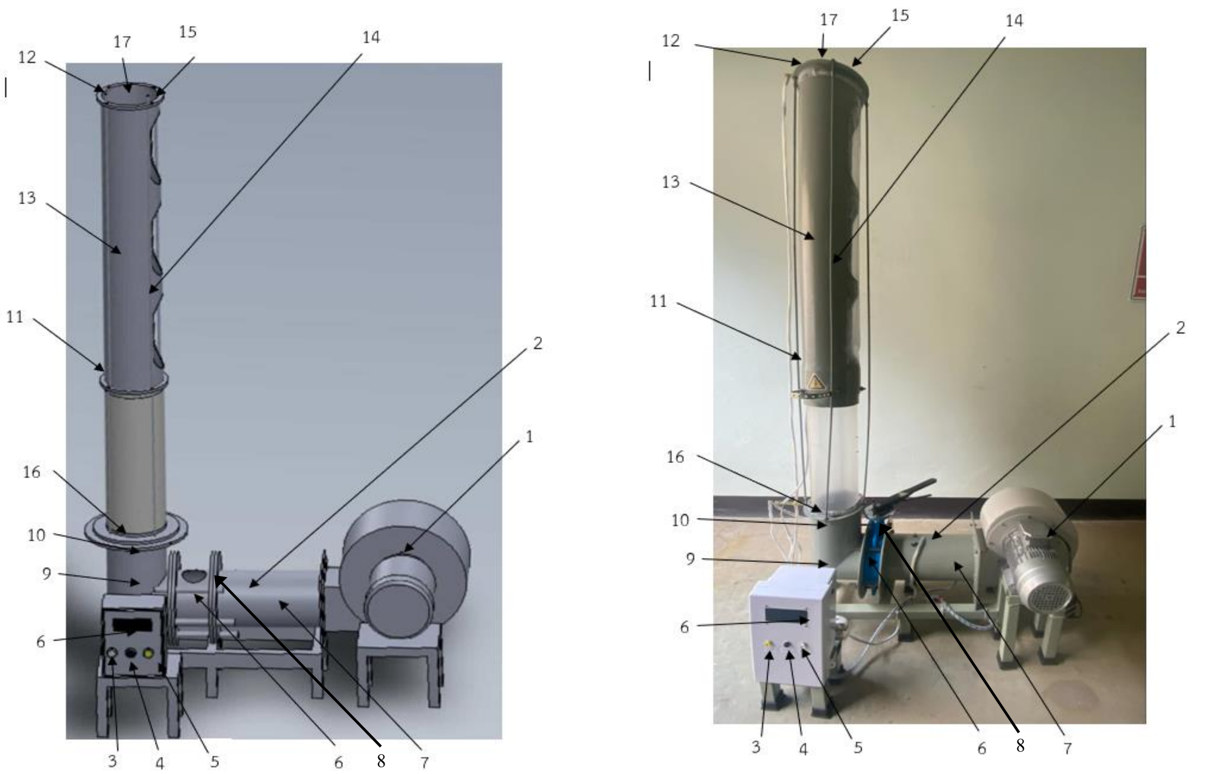

(a) (b)

1 Blower
2 Heating unit
3 Temperature control button 40°C
4 Temperature control button 50°C
5 Temperature control button 60°C
6 Display screen
7 Hot air straight duct
8 Butterfly valve
9 Hot air elbow (90°)
10 Temperature and Relative Humidity sensor (inlet)
11 Temperature and Relative Humidity sensor (middle)
12 Temperature and Relative Humidity sensor (outlet)
13 Drying column
14 Column support rod
15 Column support flange
16 Inlet steel mesh screen
17 Outlet steel mesh screen

Fig. 4. The designed paddy dryer: (a) solid works model and (b) actual prototype.

3.2 Results of Fluidization Velocity Testing

To determine the appropriate air velocity for fluidization, the blower speed was incrementally adjusted across five levels (3.4, 3.56, 6.48, 9.67, and 11.74 m/s) at a controlled temperature of 50 °C. The speed was increased until a 1,500 g sample of paddy rice achieved uniform fluidization, characterized by consistent particle suspension throughout the drying chamber. The corresponding air velocities were measured and recorded using a calibrated anemometer, with the details presented in Table 1.

Table 1. Effect of airflow conditions on paddy behavior in the column.

Valve level	Average air velocity (m/s)	Flow rate (m^3/s)	Re	Nu (heating, n = 0.4)	h ($W/m^2 \cdot {}^oC$)	Bed behavior
1	0.34	0.0062	47.1	0.43	4.9	No visible fluidization observed in the bed
2	3.56	0.0649	493.5	2.85	31.9	Initial movement detected at the bed edges
3	6.48	0.1184	898.2	4.6	51.5	Minor fluidization at center and periphery of the bed
4	9.67	0.1755	1340.4	6.33	70.9	Stable and uniform fluidization throughout the bed
5	11.74	0.2136	1627.4	7.4	82.8	Asymmetric fluidization initiated on one side

Air properties at approximately 50 °C: Pr = 0.70, k = 0.028 W/m·°C.,
Characteristic length: L = 0.0025 m (equivalent to the diameter of a paddy grain, ~2.5 mm).

From a fluid-mechanics perspective, the progression of bed behavior with increasing airflow velocity corresponds to a rise in the Reynolds number (Re). At low Re values, viscous forces dominate, and the drag force exerted on individual grains is insufficient to overcome their weight and interparticle friction; thus, no fluidization occurs. As Re increases, inertial effects become more significant, causing the bed to transition from edge movement to partial suspension. Near the minimum fluidization condition—observed at 9.67 m/s with a minimum Re of 1340.4—grain–air interactions reach a balance, resulting in a stable and well-mixed bed.

Once fluidization is established, convective heat transfer is enhanced. In this regime, the Nusselt number (Nu), which quantifies the relative effectiveness of convection over conduction, increases with airflow intensity and mixing efficiency. Correspondingly, the convective heat transfer coefficient (h) rises as the bed shifts from a non-fluidized to a stably fluidized state, reducing the thermal boundary layer thickness and accelerating both heat and moisture removal. At the optimal velocity of 9.67 m/s, Nu reaches 6.33 and h is 70.9 $W/m^2 \cdot °C$, representing favorable conditions for efficient drying. These findings align with established fluidization and convective heat-transfer theory [12].

3.3 Effects of Air Temperature and Relative Humidity Within the Column

This study investigated the conditions affecting moisture reduction in paddy by applying three drying temperatures (40°C, 50°C, and 60°C) and three drying durations (60, 90, and 120 minutes). Other variables were held constant, including the quantity of paddy (1,500 grams) and the airflow velocity (9.67 m/s). The experimental results concerning the variation in temperature and relative humidity (%RH) within the fluidized bed column under these conditions are detailed as follows.

3.3.1 Effects of temperature distribution within the column

At 60 minutes (Figure 5), temperatures at the mid- and outlet sections of the column rapidly reached their target within 10 minutes and remained stable, indicating uniform heat distribution and precise control via the Arduino IDE—critical for preserving the quality of temperature-sensitive crops like paddy. At 90 minutes (Figure 6), temperatures gradually increased and achieved thermal equilibrium after 15–20 minutes, reflecting improved thermal penetration that facilitates deeper moisture removal without risking overheating. However, at 120 minutes (Figure 7), temperatures slightly exceeded the setpoint near the end of the drying cycle, suggesting thermal buildup and the potential for over-drying if airflow or heat input is not properly adjusted.

Overall, the findings across the three time intervals suggest that drying duration significantly influences temperature stability and distribution within the system. The 60–90 minute range demonstrated the most stable thermal profile and efficient drying performance for paddy. These results align with the findings of Chupawa *et al*. [13] and Luthra [4], which emphasized that fluidized bed drying systems offer accurate control over temperature and humidity, ultimately enhancing grain quality and reducing kernel fissuring.

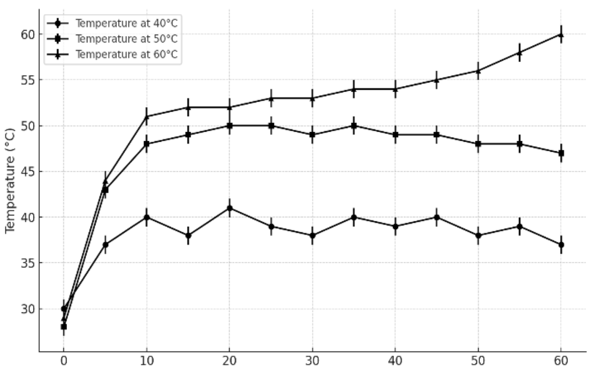

Fig. 5. Monitoring of internal column temperature during a 60-minute controlled paddy drying operation.

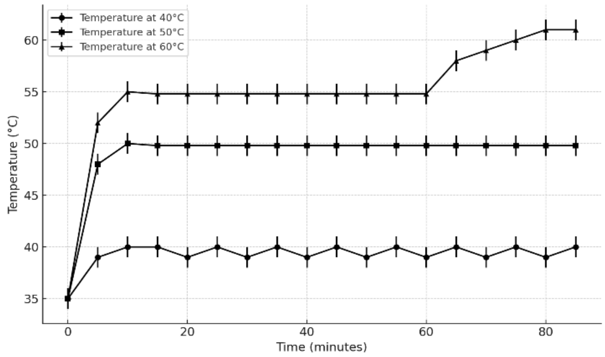

Fig. 6. Monitoring of internal column temperature during a 90-minute controlled paddy drying operation.

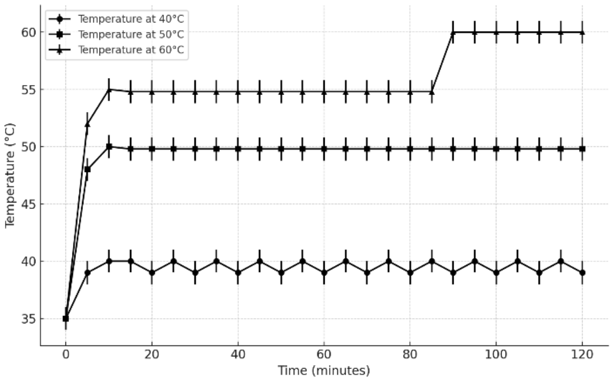

Fig. 7. Monitoring of internal column temperature during a 120-minute controlled paddy drying operation.

3.3.2 Effects of relative humidity within the column

The experimental results illustrate trends in the variation of relative humidity (%RH) within the drying column over different drying durations—60, 90, and 120 minutes—across three temperature levels (40°C, 50°C, and 60°C), as shown in Figures 8–10. A pronounced decline in %RH was observed at the beginning of each drying process, corresponding to the constant rate period, during which surface moisture evaporates rapidly. This phase primarily involves the removal of free water located on the grain surface or within interstitial spaces [4], [14]. Subsequently, the process transitions into the falling rate period, where moisture migration from the grain interior occurs more slowly [4].

At 60 minutes (Figure 8), relative humidity values measured at different positions within the column still varied considerably, particularly at lower temperatures, indicating uneven moisture removal among the paddy grains. However, as drying time increased to 90 minutes (Figure 9), %RH values across the column became more consistent, reflecting improved uniformity in moisture transfer—especially at 50°C and 60°C. By 120 minutes (Figure 10), RH values at all positions had dropped to below 20%, demonstrating that prolonged drying enhances internal moisture migration and reduces the risk of post-drying moisture reabsorption [16]–[17].

Moreover, the installation of real-time %RH sensors at three vertical points in the column significantly enhanced process analysis and control. This setup highlights the advantages of the automated fluidized bed system in delivering precise drying control, leading to high-quality results with optimized energy efficiency.

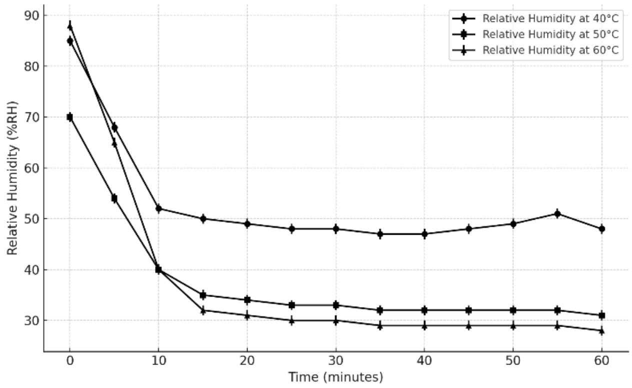

Fig. 8. Monitoring of relative humidity inside the column during a 60-minute paddy drying process.

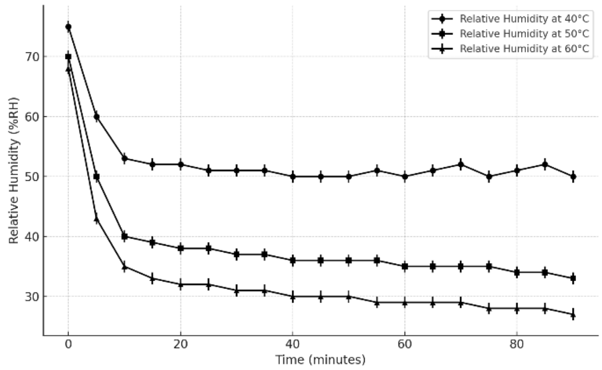

Fig. 9. Monitoring of relative humidity inside the column during a 90-minute paddy drying process.

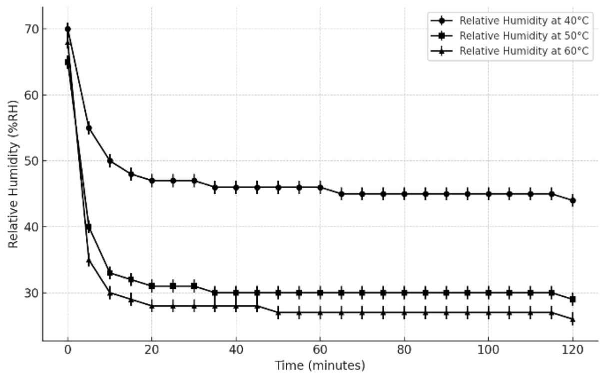

Fig. 10. Monitoring of relative humidity inside the column during a 120-minute paddy drying process.

3.4 Effect of Moisture Reduction and Specific Energy Consumption

The evaluation of moisture reduction efficiency using an automated fluidized bed drying system demonstrated that all tested temperatures (40°C, 50°C, and 60°C) and drying durations (60, 90, and 120 minutes) successfully reduced paddy moisture content to levels considered safe for storage, typically ranging between 13–16% on a dry basis [9], [18]. This range is essential for slowing quality deterioration and extending shelf life [19]. Notably, the highest moisture reduction efficiency (70.62%) was achieved at 60°C for 120 minutes, followed by 58.00% at 50°C for 120 minutes, as shown in Table 2. These results indicate a positive correlation between increased drying temperature and time and enhanced moisture removal, as higher temperatures accelerate evaporation. However, excessive heat may induce kernel fissuring and degrade grain quality [20]. Anomalously low efficiency (9.79%) was observed at 60°C for 60 minutes, suggesting the need for further investigation and better control of initial moisture content to improve the accuracy and reliability of future experiments.

Drying time significantly influenced moisture reduction ($p = 0.000$), while temperature did not ($p = 0.209$), indicating time as the primary factor. However, system performance was best explained by the interaction between temperature and time ($p < 0.001$), underscoring the need for combined control. Tukey's test showed that 40°C for 120 minutes achieved the highest reduction, whereas 60°C for 60 minutes was least effective, confirming that high temperature alone is insufficient without adequate time. These results highlight the importance of optimizing both parameters together to ensure drying efficiency and product quality.

Table 2. Moisture reduction and specific energy consumption (SEC) of paddy under varying drying temperatures and times.

Temperature (°C)	Drying Time (min)	Moisture Reduction (%)	SEC (MJ/kg)	Average SEC (MJ/kg)
40	60	$34.72^{e,f} \pm 1.32$	$25.027^{b} \pm 1.56$	28.999
	90	$31.71^{e,f} \pm 2.57$	$28.421^{c} \pm 0.53$	
	120	$37.72^{e} \pm 0.82$	$33.548^{d} \pm 1.00$	
50	60	$30.43^{f} \pm 0.78$	$18.140^{a} \pm 1.05$	20.853
	90	$43.06^{d} \pm 0.97$	$19.392^{a} \pm 1.21$	
	120	$58.00^{b} \pm 1.10$	$25.027^{b} \pm 0.68$	
60	60	$9.79^{g} \pm 3.67$	$17.080^{a} \pm 0.77$	20.942
	90	$52.93^{c} \pm 1.00$	$18.377^{a} \pm 0.85$	
	120	$70.62^{a} \pm 1.42$	$27.368^{b,c} \pm 1.07$	

Values with the different superscripts in each row are significantly different ($p \leq 0.05$).

Energy consumption during drying was assessed using specific energy consumption (SEC), a key performance metric in energy and process engineering. SEC is influenced by drying technology, system scale, temperature, airflow, and initial moisture content [21]–[22].

In this study, both temperature and drying time had significant effects on SEC ($p < 0.001$), with significant interaction between them ($p = 0.013$). SEC decreased with longer drying durations, particularly at 60°C, where the lowest value (17.08 MJ/kg) was recorded. In contrast, the highest SEC (33.55 MJ/kg) occurred at 40°C for 120 minutes, reflecting higher energy demand at low temperatures and extended drying. Tukey's test confirmed significant differences among temperature–time combinations.

These findings are directly relevant to SDG 7: Affordable and Clean Energy, as they demonstrate that careful selection of drying parameters can maximize moisture removal while minimizing energy use. The condition of 60°C for 120 minutes provided the highest moisture reduction with moderate energy consumption, representing a balance between operational efficiency and sustainable energy use. Such optimization not only supports product quality but also aligns with global efforts to improve energy efficiency in agricultural processing, particularly for medium-scale farms and small-scale agro-industrial operations seeking cost-effective and environmentally responsible drying solutions.

4. CONCLUSION

An automated fluidized bed dryer with Arduino-based temperature and humidity control was developed and evaluated to enhance energy efficiency in agricultural drying, aligning with SDG 7: Affordable and Clean Energy. Although statistical analysis revealed no significant differences in moisture reduction or specific energy consumption (SEC) across operating conditions, experimental trends were evident. Drying at 60 °C for 120 minutes achieved the highest performance, with substantial moisture reduction (70.62%) and moderate energy use (27.37 MJ/kg), demonstrating a favorable balance between operational effectiveness and energy conservation. This makes it a suitable condition for practical application in drying 1,500 g of paddy at 14.35% initial moisture content, while contributing to sustainable postharvest practices and global energy efficiency goals. Future work should focus on increasing batch capacity and improving control system stability to further enhance operational sustainability.

ACKNOWLEDGEMENT

The authors gratefully acknowledge the Faculty of Engineering, Rajamangala University of Technology Lanna, for providing essential laboratory facilities, research instrumentation, and academic support. Appreciation is also extended to the research team and laboratory staff for their contributions to system design, equipment validation, and data analysis, all of which were integral to the successful execution and completion of this study.

NOMENCLATURE

$MC_{w.b.}$	= moisture content (wet basis)
w_w	= weight of water (kg)
w_d	= dry weight of the material (kg)
Q	= heat transfer rate (kW)
h	= convective heat transfer coefficient (W/m²·°C)
A	= surface area (m^2)
T_{air}	= temperature of the air (°C)
$T_{surface}$	= temperature of the grain surface (°C)
Nu	= Nusselt number
Re	= Reynolds number
Pr	= Prandtl number
L	= characteristic length (m)
c_p	= specific heat capacity (J/kg· °C)
k	= thermal conductivity (W/m·°C)
SEC	= specific energy consumption (MJ/kg of water)
E	= total energy input from the blower and electric heater (MJ)
m_w	= mass of water evaporated (kg)

Greek symbols

ρ	= density (kg/m^3)
μ	= dynamic viscosity (kg/m·s)

REFERENCES

[1] Tiwari G.N. and S. Sarkar. 2020. Review on recent advances in solar drying technologies for agricultural produce. *Renewable and Sustainable Energy Reviews* 122: 109734.

[2] Anwar S., Rehman F., and Khan I., 2021. Performance analysis of hybrid solar-electric dryer for agricultural products. *Renewable Energy Focus* 38: 52–61.

[3] Ying C. and R. Spang. 2024. Comparative energy analysis of paddy drying technologies in Southeast Asia. *Renewable Agriculture and Food Systems* 39(1):120–129. https://doi.org/10.1017/raf.2023.45.

[4] Luthra K., 2021. Developing a lab-scale fluidized bed dryer system to enhance rough rice drying process. MS Thesis (published). University of Arkansas, Fayetteville,USA. https://scholarworks.uark.edu/etd/4138.

[5] Wazed M.A., Mozumder N.H.M.R., and Sarker M.S.H., 2022. Head rice yield of paddy dried in two stage and conventional drying methods. *Agricultural Engineering International: CIGR Journal* 24(3): 190–200.

[6] Choicharoen K., 2024. Energy efficiency of paddy dehydration process using vortex dryer. *Journal of Food Process Engineering* 14(4): 99–107.

[7] Nebrida A.P., 2024. Smart integration in agriculture: An Arduino-driven rice grain dryer for optimal post-harvest management. *Journal of Electrical Systems and Information Technology* 11: 46. https://doi.org/10.1186/s43067-024-00170-0.

[8] Herani N., Rahmat S., and Prasetia V., 2023. Monitoring of rice dryer machine using tray dryer method. *Infotekmesin* 14(2): 311–317. https://doi.org/10.35970/infotekmesin.v14i2.1915.

[9] Çengel Y.A. and A.J. Ghajar. 2020. *Heat and mass transfer: Fundamentals and applications* (6th ed.). New York: McGraw-Hill Education.

[10] Joycharoen K., 2020. Performance and energy consumption study of a swirl-fluidized bed dryer for paddy. Master's Thesis, King Mongkut's University of Technology North Bangkok, Bangkok, Thailand.

[11] Wormsbecker M., Pugsley T., and Tanfara H., 2016. The influence of distributor design on fluidized bed dryer hydrodynamics. In *Proceedings of the 12th International Conference on Fluidization*, Gyeong-ju, Korea, 22–27 May.

[12] Kunii D. and O. Levenspiel. 1991. *Fluidization engineering* (2nd ed.). Oxford: Butterworth-Heinemann.

[13] Chupawa P., Gaewsondee T., and Duangkhamchan W., 2021. Drying characteristics and quality attributes affected by a fluidized-bed drying assisted with swirling compressed-air for preparing instant red jasmine rice. *Processes* 9(10): 1738. https://doi.org/10.3390/pr9101738.

[14] Ayensu A., 1997. Dehydration of food crops using a solar dryer with convective heat flow. *Solar Energy* 59: 121–126. https://doi.org/10.1016/S0038-092X(96)00130-2.

[15] Yiotis A., Tsimpanogiannis I., Stubos A., and Yortsos Y., 2006. Pore-network study of the characteristic periods in the drying of porous materials. *Journal of Colloid and Interface Science* 297(2): 738–748. https://doi.org/10.1016/j.jcis.2005.11.043.

[16] Li G., Kaixuan X., Qichao Y., Yuangyang Z., and Liansheng L., 2022. Flow field and drying process analysis of double-layer drying chamber in heat pump dryer. *Applied Thermal Engineering* 118261. https://doi.org/10.1016/j.applthermaleng.2022.118261.

[17] Aranha A., Ferrari A.L., Bissaro C.A., Matias G., Defendi R., Paschoal S.M., and Jorge L.M., 2023. Mathematical modelling of wheat drying by fractional order and assessment of transport

properties. *The Canadian Journal of Chemical Engineering*. https://doi.org/10.1002/cjce.25081.

[18] Yahya M., Fahmi H., Fudholi A. and Sopian K., 2018. Performance and economic analyses on solar-assisted heat pump fluidised bed dryer integrated with biomass furnace for rice drying. *Solar Energy* 174: 1058-1067. https://doi.org/10.1016/j.solener.2018.10.002.

[19] Zhu D., Wang T., Liu X., Bi J., Zhang W., Zeng X., Wang P., and Shu Z., 2024. Quality changes in Chinese high-quality Indica rice under different storage temperatures with varying initial moisture contents. *Frontiers in Nutrition* 11: 1334809. https://doi.org/10.3389/fnut.2024.1334809.

[20] Ondier G., Siebenmorgen T., and Mauromoustakos A., 2010. Low-temperature, low-relative humidity drying of rough rice. *Journal of Food Engineering* 100: 545–550. https://doi.org/10.1016/j.jfoodeng.2010.05.004.

[21] Mondal M.H.T. and M.S.H. Sarker. 2024. Comprehensive energy analysis and environmental sustainability of industrial grain drying. *Renewable and Sustainable Energy Reviews* 114442. https://doi.org/10.1016/j.rser.2024.114442.

[22] Ying T. and E. Spang. 2024. Paddy drying technologies: A review of existing literature on energy consumption. *Processes* 12(3): 532.